Atmos. Meas. Tech. Discuss., 6, 8603–8645, 2013
www.atmos-meas-tech-discuss.net/6/8603/2013/
doi:10.5194/amtd-6-8603-2013

Atmospheric Measurement Techniques Discussions
Open Access

Validation of SCIAMACHY O_2 A band cloud heights using Cloudnet radar/lidar measurements

P. Wang and P. Stammes

Royal Netherlands Meteorological Institute (KNMI), De Bilt, the Netherlands

Received: 16 July 2013 – Accepted: 6 September 2013 – Published: 1 October 2013

Correspondence to: P. Wang (ping.wang@knmi.nl)

Published by Copernicus Publications on behalf of the European Geosciences Union.

Validation of SCIAMACHY O_2 A band cloud heights

P. Wang and P. Stammes

Abstract

For the first time two SCIAMACHY O_2 A band cloud height products are validated using ground-based radar/lidar measurements between January 2003 and December 2011. The products are the ESA Level 2 (L2) version 5.02 cloud top height and the FRESCO (Fast Retrieval Scheme for Clouds from the Oxygen A band) version 6 cloud height. The radar/lidar profiles are obtained at the Cloudnet sites of Cabauw and Lindenberg, and are averaged for one hour centered at the SCIAMACHY overpass time to achieve an optimal temporal and spatial match. In total we have about 220 cases of single layer clouds and 200 cases of multi-layer clouds. The FRESCO cloud height and ESA L2 cloud top height are compared with the Cloudnet cloud top height and Cloudnet cloud middle height. We find that the ESA L2 cloud top height has a better agreement with the Cloudnet cloud top height than the Cloudnet cloud middle height. The ESA L2 cloud top height is on average 0.44 km higher than the Cloudnet cloud top height, with a standard deviation of 3.07 km. The FRESCO cloud height is closer to the Cloudnet cloud middle height than the Cloudnet cloud top height. The mean difference between the FRESCO cloud height and the Cloudnet cloud middle height is −0.14 km with a standard deviation of 1.88 km. The SCIAMACHY cloud height products are further compared to the Cloudnet cloud top height and the Cloudnet cloud middle height in 1 km bins. For single layer clouds, the difference between the ESA L2 cloud top height and the Cloudnet cloud top height is less than 1 km for each cloud bin at 3–7 km, which is 24 % percent of the data. The difference between the FRESCO cloud height and the Cloudnet cloud middle height is less than 1 km for each cloud bin at 0–6 km, which is 85 % percent of the data. The results are similar for multi-layer clouds, but the percentage of cases having a bias within 1 km is smaller than for single layer clouds. Since globally about 60 % of all clouds are low clouds and 42 % are single-layer low clouds, we expect that globally for a large percentage of cases the FRESCO cloud height would be close to the cloud middle height.

AMTD

6, 8603–8645, 2013

Validation of SCIAMACHY O_2 A band cloud heights

P. Wang and P. Stammes

1 Introduction

The SCIAMACHY instrument had performed measurements of trace gases, clouds and aerosols for almost 10 yr (2002–2012) when Envisat and its payload stopped operations unexpectedly on 8 April 2012. SCIAMACHY measured the reflected Earth radiance and incident solar irradiance at the top of the atmosphere in the 240–1750 nm wavelength range at a spectral resolution of 0.2–1.5 nm (Bovensmann et al., 1999). It is a challenge to retrieve cloud information from SCIAMACHY because of its large pixel size. In an area of 60 km × 30 km, which is the typical SCIAMACHY pixel size for the O_2 A band wavelength range, clouds are often multi-layer, inhomogeneous, or broken.

Clouds affect trace gas retrievals from SCIAMACHY and other instruments, because of shielding of the lower atmosphere, enhanced sensitivity above clouds (albedo effect), and in-cloud absorption. Cloud height, cloud fraction and cloud optical thickness are all important for cloud correction of trace gas retrievals, especially for trace gases in the troposphere (Boersma et al., 2004; Stammes et al., 2008). Regarding climate studies, clouds play an important role in the energy and water cycle of the Earth. A change of only about 1 % in global cloudiness can either mask or double the effect that a decade's worth of greenhouse-gas emissions have on the amount of Earth's heat lost to space (Wielicki et al., 2005).

Within the Global Energy and Water Experiment (GEWEX) Cloud Assessment project (Stubenrauch et al., 2012) various satellite-derived monthly mean global cloud products were compared. From this intercomparison of cloud observations from multispectral imagers, multi-angle multi-spectral imagers, IR sounders and lidar, Stubenrauch et al. (2012) concluded that cloud top height can be accurately determined with lidar (e.g. CALIPSO; Winker et al., 2009) whereas passive remote sensing provides a "radiative height" (apart from the MISR stereoscopic height retrieval). In general, the "radiative height" lies near the middle between cloud top and "apparent" cloud base. When cloud height is determined via O_2 absorption (e.g. POLDER; Ferlay et al., 2010), it corresponds to a location even deeper inside the cloud. The height-stratified

AMTD
6, 8603–8645, 2013

cloud amount was determined for high, middle and low clouds, with separation levels at 440 hPa and 680 hPa, corresponding to altitudes of about 6 km and 3 km, respectively. Stubenrauch et al. (2012) found that about 42 % of all clouds are high-level clouds with optical depth > 0.1; the fraction of high clouds decreases to 20 % when considering only clouds with optical depth > 2. About 16 % (±5 %) of all clouds correspond to mid-level clouds with no other clouds above. About 42 % (±5 %) of all clouds are single-layer low-level clouds. When including low-level clouds underneath semi-transparent higher level clouds, about 60 % of all clouds correspond to low-level clouds.

The radar/lidar combination can be considered as being currently the most accurate remote sensing tool to measure cloud vertical extent. However, these active instruments have necessarily a very small field-of-view (FOV). The ground-based radar/lidar instruments often point to the zenith only, whereas the CALIPSO and Cloudsat instruments have small footprints and narrow swaths on the Earth's surface. Therefore, most of the time passive satellite instruments (imaging radiometers or spectrometers) and active satellite-based or ground-based instruments observe different (parts of) clouds. Since the comparison between cloud top height from passive satellite instruments and radar/lidar instruments requires a good temporal and spatial matching, the small FOV of radar/lidar limits the amount of data available for the intercomparison. A larger validation data set would give better statistics and would lead to more significant conclusions on the accuracy of cloud height retrievals from passive instruments.

We obtained this large radar/lidar cloud height validation data set from the Cloudnet project. The Cloudnet project (Illingworth et al., 2007) operates a network of ground-stations to continuously monitor cloud-related variables over multi-year time periods. The remote sensing sites of Cabauw and Lindenberg are two Cloudnet sites which are equipped with suitable ground-based remote sensing instruments, such as radar, lidar, and microwave radiometer, to measure cloud and aerosol profiles operationally (www.cloud-net.org). The time period of the Cloudnet products covers the whole lifetime of SCIAMACHY (2002–2012), which provides a unique opportunity to validate the whole time series of SCIAMACHY cloud height products.

AMTD
6, 8603–8645, 2013

The Fast Retrieval Scheme for Clouds from the Oxygen A band (FRESCO) is an operational cloud retrieval algorithm developed by Koelemeijer et al. (2001) and Wang et al. (2008), which derives effective cloud fraction and cloud height from GOME, SCIAMACHY and GOME-2 O_2 A band observations and provides near-real-time data to users via the TEMIS web site (http://www.temis.nl). The FRESCO cloud algorithm (version 5) was validated using ground-based radar/lidar cloud observations at the SGP/ARM site for one year of data (Wang et al., 2008). They reported that the FRESCO retrieved cloud height was close to the mid-level of the clouds. Recently, the FRESCO algorithm (version 6, Wang et al., 2012) has been improved by using the MERIS surface albedo database (Popp et al., 2011) and O_2 line parameters from HITRAN 2008 (Rothman et al., 2009).

The cloud top height in the SCIAMACHY ESA Level 2 (L2) operational product is derived from the O_2 A band using SACURA (SemiAnalytical CloUd Retrieval Algorithm; Rozanov and Kokhanovsky, 2004; Kokhanovsky et al., 2006). For partly cloud pixels, first the cloud fraction is retrieved using OCRA (Optical Cloud Recognition Algorithm; Loyola, 2004) and then the cloud top height is derived. The SACURA algorithm implemented in the ESA L2 processor is a fast version of the scientific SACURA algorithm. Cloud top heights derived from GOME and SCIAMACHY measurements using the scientific SACURA algorithm have been compared with ground-based and satellite measurements for limited data sets and time periods (Kokhanovsky et al., 2006, 2007; Rozanov et al., 2006). Recently Lelli et al. (2012) compared GOME cloud top heights retrieved using the scientific SACURA algorithm with cloud top heights from radar/lidar measurements at Atmospheric Radiation Measurement (ARM) sites and Chilbolton for 51 cases. They found that the GOME cloud top height from SACURA was higher than the radar-measured cloud top for shallow clouds and lower than the radar-measured cloud top for deep clouds. Here deep clouds refer to clouds of which the top is higher than 3 km and the vertical extent is greater than 50 % of its height; other clouds are referred to as shallow clouds (Sayer et al., 2012).

AMTD
6, 8603–8645, 2013

The SCIAMACHY ESA L2 cloud product has been compared before with the FRESCO cloud product and the SACURA scientific product (Lichtenberg, 2009). However, the quality of L2 product is not only determined by the retrieval algorithm but also by the quality of the level 1 (L1) product used as input. In this paper the latest SCIAMACHY ESA L1 product (version 7.04) is used for both cloud products, namely the ESA L2 product version 5.02 and the FRESCO product version 6. This is the first time that the full time series of the latest SCIAMACHY ESA L2 cloud top height and FRESCO cloud height products are being validated with the same independent ground-based radar/lidar measurements.

In Sect. 2 we describe the validation data set. Section 3 contains the methodology for the validation. The results are presented in Sect. 4. Conclusions are drawn in Sect. 5.

2 Data sets

2.1 SCIAMACHY FRESCO cloud product

FRESCO has been developed as a simple, fast, and robust algorithm to provide cloud information for cloud correction in trace gas retrievals, such as ozone and NO_2 (Koelemeijer et al., 2001; Wang et al., 2008). FRESCO uses the reflectances in three 1 nm wide windows of the O_2 A band: 758–759 nm, 760–761 nm, and 765–766 nm. In FRESCO the cloud is assumed to be a Lambertian reflector with albedo 0.8. Only O_2 absorption along the light path and single Rayleigh scattering are taken into account; absorption by oxygen inside the cloud is neglected. The transmission in the O_2 A band is first calculated line-by-line based on the O_2 line parameters in the HITRAN 2008 database (Rothman et al., 2009) and then convolved with the SCIAMACHY spectral response function (slit function). Surface albedo is an a-priori parameter for FRESCO retrievals, and is taken from the MERIS monthly climatological surface albedo data base (Popp et al., 2011). For a partly cloudy pixel, the reflectance is assumed to be the sum of the reflectances from the clear-sky part and the cloudy part of the pixel.

The retrieved cloud parameters are the effective cloud fraction (between 0 and 1) and the cloud pressure. The O_2 transmission and Rayleigh scattering are calculated using the mid-latitude summer (MLS) atmospheric profile (Anderson, 1986); therefore, cloud pressure can be converted into cloud height (and vice-versa) using the MLS atmospheric profile.

2.2 SCIAMACHY ESA level 2 cloud product

The SCIAMACHY ESA level 2 (L2) cloud top height is derived using the SACURA algorithm. SACURA determines the cloud top pressure and cloud optical thickness using measurements of the cloud reflectance in the entire O_2 A band at 756–770 nm (Rozanov and Kokhanovsky, 2004). The forward model simulates the reflectance at top-of-atmosphere (TOA), assuming clouds to be a scattering layer and including multiple scattering and oxygen absorption above, below and inside the clouds, as well the surface reflection contribution. The SACURA algorithm is based on an analytical approximation of the reflectance for optically thick clouds (optical thickness $\tau > 5$), therefore the algorithm is much faster than an exact radiative transfer simulation. For broken clouds extra information on the cloud fraction is required which can be obtained using OCRA, discussed below. The reflectance at TOA is assumed to be the sum of the reflectance from the cloud-free part of the pixel and the cloudy part of the pixel weighted by the cloud fraction. For the retrieval algorithm, in order to find the cloud top height (h), the TOA reflectance is presented in the form of a Taylor expansion around the a-priori assumed value of cloud top height (h_0). The assumed cloud top height is 1 km in SACURA, which is a typical value for low clouds (Feigelson, 1981). Neglecting the nonlinear term, the cloud height is obtained from the fit to the measured reflectances in the O_2 A band. The main assumption in SACURA is that the relationship between reflectance and cloud top height can be presented by a linear function on the interval (h–h_0). The oxygen absorption cross-sections are calculated from a correlated k-distribution method (Buchwitz et al., 2000). The SACURA algorithm was implemented in the SCIAMACHY ESA L2 processor at DLR (German Space Agency). The ESA

AMTD
6, 8603–8645, 2013

L2 cloud product is described in the SCIAMACHY L2 products Algorithm Theoretical Baseline Document (Lichtenberg, 2011).

The ESA L2 operational cloud fraction is retrieved using the Optical Cloud Recognition Algorithm (OCRA) which is a PMD (Polarization Measurement Device) algorithm using the red, green and blue PMDs for cloud fraction determination (Loyola, 2004). The basic idea of OCRA is to decompose the radiance measured by an optical sensor into two components: the background and the clouds. The PMD radiances in the red (PMD3), green (PMD2) and blue (PMD1) are calculated and normalized by the sum of the three radiances. The cloud-free composite is created by selecting the pixels with minimum radiance out of the multi-temporal data set. The fractional cloud cover, defined in the range [0, 1], is determined from the distance between the measured radiance and the cloud-free radiance. However, the cloud fraction also depends on scaling and offset factors that are proportional to the position of the white point [1/3, 1/3, 1/3] in the RGB-space.

2.3 Cloudnet target classification product

Cloudnet is a network of ground-based remote sensing sites for the continuous evaluation of cloud and aerosol profiles in operational numerical weather prediction models. These sites provide vertical profiles of cloud cover and cloud ice and liquid water contents at high spatial and temporal resolution by using active sensors such as lidar and Doppler millimeter-wave radar. In order to retrieve cloud microphysical properties, the backscatter targets in each of the radar/lidar pixels have to be categorized into different classes (Illingworth et al., 2007).

The vertically pointing Doppler cloud radar and backscatter lidar are the most relevant instruments for the Cloudnet target classification (Hogan and O'Connor, 2004). The radar can detect rain, drizzle drops, ice particles and insects, because it is sensitive to large particles. Cloud droplets and aerosols can be identified from lidar measurements, because the lidar is sensitive to small particles (Illingworth et al., 2007). In the target classification product, each radar/lidar backscatter pixel is classified as liquid

AMTD
6, 8603–8645, 2013

droplets, ice, insects, aerosols, clear-sky, or other categories. The target classification product also contains cloud top height and cloud base height. Cloud top and cloud base height correspond to the highest and lowest backscatter pixels, respectively, that have clouds. Therefore, for multi-layer clouds, the cloud top and cloud base height do not refer to the same clouds. An example of the Cloudnet target classification product at Lindenberg (Germany) is shown in Fig. 1. At Cabauw (the Netherlands) the target classification product is produced every 15 s at 90 m vertical resolution. At Lindenberg, the cloud profile has a time resolution of 30 s and a vertical resolution of 30 m. A summary of the Cloudnet target classification product at Cabauw and Lindenberg is given in Table 1.

3 Methodology

The FRESCO and ESA L2 cloud products are processed using the same SCIAMACHY L1 data. The SCIAMACHY FRESCO and ESA L2 global cloud products are first intercompared to show the general features of the O_2 A band cloud retrievals and to give more statistics. Next, the validation is performed using collocated SCIAMACHY data and Cloudnet radar/lidar measurements.

The Cloudnet target classification product and cloud boundaries at Cabauw and Lindenberg are used for the validation of SCIAMACHY cloud height products, because they have long continuous data sets: from January 2001 to June 2005 at Cabauw and from January 2005 until now at Lindenberg. Therefore, the combination of these two sites covers the whole SCIAMACHY mission period. For the validation the Cloudnet and SCIAMACHY measurements from January 2003 to December 2011 are used to construct a collocated data set.

For every SCIAMACHY pixel covering Cabauw or Lindenberg, one hour of Cloudnet target classification data, centered at the SCIAMACHY overpass time, is selected as collocated data. Thus, for every cloud height measurement from SCIAMACHY there are about 240 (temporal) × 126 (vertical) radar/lidar backscatter pixels at Cabauw and

AMTD
6, 8603–8645, 2013

120 (temporal) × 450 (vertical) radar/lidar backscatter pixels at Lindenberg, which are classified as one of the 10 categories or clear-sky. The categories "ice" and "cloud droplets only" are used to determine ice and water clouds (see Fig. 1). The categories with "drizzle" and "rain" usually occur at the cloud base, so they have no impact on the SCIAMACHY cloud retrievals. These cases with precipitation are included in the validation data set. Height distributions of the radar/lidar backscatter pixels are derived for ice clouds, water clouds, and both types, respectively, from 250 m to 12 000 m with a bin size of 270 m. Some examples of cloud height distributions are shown in Fig. 2. If the distribution has a single mode without interruption by clear-sky pixels, the cloud case is classified as a single-layer cloud. If more than one mode appears in the distribution and these modes are separated by clear-sky pixels, the case is classified as a multi-layer cloud. As illustrated in Fig. 2, single layer cloud A has a single peak, whereas single layer cloud B has two peaks; but since there are no clear-sky pixels between the two peaks, case B is classified as a single layer cloud.

The validation is performed separately for single-layer clouds and multi-layer clouds, because in the SACURA and FRESCO cloud retrieval algorithms clouds are assumed to be single layers. Water and ice clouds have different scattering matrices, therefore the single layer clouds are further separated into water and ice clouds. The Cloudnet cloud top height is the arithmetic mean of the cloud top heights in a 1 h period around the SCIAMACHY overpass time; the same holds for the cloud base height. For single-layer clouds we compare the Cloudnet cloud top and cloud base heights with the SCIAMACHY cloud heights. For multi-layer clouds, we define a "cloud middle height" which is the arithmetic mean of all the radar/lidar cloudy backscatter pixel heights. The cloud middle height depends on the cloud height distribution; it often differs from the mean of cloud top and cloud base heights.

In the validation of FRESCO and ESA L2 cloud heights using the Cloudnet data, we are mainly focusing on the scenes having effective cloud fractions larger than 0.1. This criterion is necessary because the ESA L2 cloud top heights are often not retrieved for scenes having effective cloud fraction smaller than 0.1.

AMTD
6, 8603–8645, 2013

4 Results

4.1 Global intercomparison of FRESCO and ESA L2 cloud products

In order to present a global view of the SCIAMACHY FRESCO and ESA L2 cloud products, the FRESCO and ESA L2 cloud products are compared using a data set which consists of one orbit per month from the entire SCIAMACHY mission period and 4 full days of global data. Although the ESA L2 cloud fraction is derived from PMDs, the cloud fraction in the L2 cloud product is provided for the same pixel as the cloud top height, which is derived from the spectrometer's O_2 A-band channel. The collocation of SCIAMACHY FRESCO and ESA L2 cloud products is determined from the measurement time. The collocated data are only for SCIAMACHY pixels without snow/ice on the surface. This is because FRESCO only retrieves effective cloud fraction and cloud pressure (cloud height) for non-snow/ice pixels. For snow/ice pixels, FRESCO assumes a cloud fraction of 1 and retrieves the scene albedo and the scene pressure. The data set has in total about 9×10^5 collocated data points for (effective) cloud fraction and 6×10^5 for cloud (top) height. Because of non-convergence in the SACURA retrievals, the amount of collocated cloud (top) height data is less than the amount of cloud fraction data. The global frequency distributions of the FRESCO cloud height and ESA L2 cloud top height are shown in Fig. 3a. Both cloud height distributions have a maximum at 1–2 km, which indicates the global dominance of low clouds. The FRESCO mean cloud height is lower than the ESA L2 mean cloud top height due to the difference between the FRESCO and SACURA algorithms. Both algorithms retrieve the cloud height from the amount of O_2 absorption at 760 nm, which determines the length of the light path above the cloud and inside the cloud. Multiple scattering in the cloud is taken into account in the SACURA algorithm but not in the FRESCO algorithm. In FRESCO the light path of photons inside the cloud is added to the light path above the cloud. Therefore, FRESCO retrieves a lower cloud height than SACURA. In fact, FRESCO effectively retrieves a cloud mid-level height (Wang et al., 2008). The ESA L2 cloud top height distribution is cut off at 1 km as the lowest value, which is a feature of

AMTD
6, 8603–8645, 2013

the SACURA algorithm. The FRESCO effective cloud fraction and the ESA L2 cloud fraction, shown in Fig. 3b, have similar distributions except at effective cloud fractions less than 0.2. In that range the ESA L2 cloud fraction product is sharper peaked (more cloud-free pixels), whereas the FRESCO effective cloud fraction product has a wider distribution. Because the cloud fraction in the ESA L2 product is derived from PMDs which have a pixel size of about 7 km × 30 km, it has slightly more clear-sky pixels than FRESCO (Krijger et al., 2007). This may cause differences between ESA L2 cloud fraction and FRESCO effective cloud fraction at small cloud fractions. The global statistics of the FRESCO and ESA L2 cloud products are summarized in Table 2.

4.2 Validation

From January 2003 to December 2011, there are 693 collocated SCIAMACHY and Cloudnet measurements, of which 157 cases are excluded because of almost cloud-free conditions (Cloudnet cloud fraction < 0.05). In the remaining 536 cases, 297 cases are single-layer clouds and 239 cases are multi-layer clouds. The single-layer cloud cases with FRESCO effective cloud fraction > 0.1 (217 cases) include 71 cases of water clouds (class "cloud droplets only"), 103 cases of ice clouds (class "ice"), and 43 cases having co-existing water and ice clouds. For the multi-layer clouds, ice and water clouds are not analyzed separately, because most multi-layer clouds have both ice and water cloud droplets. The number of cloud-free cases is 99 according to the Cloudnet products. According to the ESA L2 product there are 82 cloud-free cases. This difference can occur due to errors in the satellite cloud detection technique, and due to partial collocation, e.g. if the Cloudnet site is located at the edge of the SCIAMACHY pixel. For the cloud-free pixels in the ESA L2 cloud product, the mean of the FRESCO effective cloud fractions is 0.0244. This is in good agreement with the global difference of 0.0225 between the FRESCO and ESA L2 cloud fractions (see Table 2).

AMTD
6, 8603–8645, 2013

4.2.1 Single-layer clouds

Figure 4 shows the scatter plots of the FRESCO cloud height vs. the Cloudnet cloud top height for all collocated single-layer clouds, single-layer water clouds and single-layer ice clouds. The color scale indicates the FRESCO effective cloud fraction. The sum of ice cloud cases and water cloud cases is smaller than the total number of cases, because some single-layer clouds having both ice and water droplets. If the FRESCO effective cloud fraction is less than 0.1, the FRESCO cloud heights show large scatter. FRESCO cloud heights are in good agreement with Cloudnet cloud top heights for low clouds, but are lower than the Cloudnet cloud top heights for high clouds. This behavior does not depend on the effective cloud fraction.

The ESA L2 cloud top height is plotted vs. the Cloudnet cloud top height for all collocated single-layer clouds in Fig. 5. The color scale indicates the ESA L2 cloud fraction (derived from OCRA). Cloud top heights of water clouds are usually below 4 km in the Cloudnet measurements. The ESA L2 cloud top height tends to be higher than the water cloud top height; however, the agreement seems to be better for low ice clouds. There is no ESA L2 cloud top height retrieval for effective cloud fractions less than 0.1. In some cases the ESA L2 cloud algorithm does not converge; therefore its cloud top height product has less data than the FRESCO cloud height product. Figure 5a shows that the L2 cloud top height tends to be higher than the Cloudnet cloud top height for small cloud fractions and lower than the Cloudnet cloud top height for large cloud fractions.

For single-layer clouds, the Cloudnet product provides accurate information of cloud top and cloud base heights. Figure 6 shows the single-layer cloud cases sorted according to the Cloudnet cloud top height. The grey bar marks the Cloudnet cloud vertical range from cloud base height to cloud top height. The red and blue points indicate the FRESCO cloud height and ESA L2 cloud top height, respectively. These are the same single-layer cloud cases as in Figs. 4 and 5, but excluding the cases which have FRESCO effective cloud fraction less than 0.1. For the cases in Fig. 6, the mean and

AMTD

6, 8603–8645, 2013

median of the (geometric) cloud fraction derived from the Cloudnet measurements are, respectively, 0.84 and 0.99. The mean variations (standard deviation) of cloud top and cloud base height are both about 340 m and of the medians about 220 m. As shown in Fig. 6, the ESA L2 cloud top height is higher than the FRESCO cloud height and sometimes even higher than the Cloudnet cloud top height. Most FRESCO cloud heights and ESA L2 cloud top heights are above the cloud base heights. For high thin clouds, both FRESCO and ESA L2 cloud heights can sometimes be below the Cloudnet cloud base heights. For high thin clouds, many photons can reach the surface before being reflected back to space. This light path is missing in FRESCO. Furthermore, the amount of O_2 absorption in scenes with thin cirrus can be very close to that of cloud-free scenes. Therefore, any small errors in the simulated O_2 absorption would cause the retrieval not to converge or yield a cloud height close to the surface. This has been shown in retrieval simulations and validations (Lelli et al., 2012; Rozanov et al., 2006).

In order to get more detailed statistics, SCIAMACHY cloud heights and Cloudnet cloud heights for single-layer clouds have been analyzed for vertical bins. The Cloudnet cloud top heights are divided into 1 km bins from 0 to 8 km, a bin for 8–10 km and a bin above 10 km. For every Cloudnet cloud top height bin, the corresponding FRESCO cloud heights and ESA L2 cloud top heights are selected and the mean and standard deviation are calculated. The results are presented in histograms in Fig. 7. The number of cases in each bin is the same for the Cloudnet data and FRESCO data, while the number of cases for ESA L2 data is generally less because of non-convergence. Therefore, the number of Cloudnet cloud data in every bin used to compare with ESA L2 cloud top height is less than that used to compare with FRESCO cloud height. In Figs. 7 and 11, only Cloudnet cloud height for collocated FRESCO cloud height is shown. The Cloudnet cloud height for collocated ESA L2 cloud top height is provided in the tables in Appendix. The As shown in Fig. 7a, below 4 km FRESCO cloud height is close to the Cloudnet cloud top height; the differences are between 0.20 km (bin 2) and −0.57 km (bin 4), which include 62 % of 217 cases. The ESA L2 cloud top height is close to the Cloudnet cloud top height for the bins at 4–7 km; the differences are

Discussion Paper | Discussion Paper | Discussion Paper | Discussion Paper |
AMTD
6, 8603–8645, 2013
Validation of SCIAMACHY O_2 A band cloud heights
P. Wang and P. Stammes

between −0.04 km (bin 5) and 0.72 km (bin 4), which include 24 % of 174 cases. However, the mean difference between ESA L2 and Cloudnet cloud top heights is small: the ESA L2 cloud top height is only 0.44 km higher than the Cloudnet cloud top height, with a standard deviation of 3.07 km. FRESCO cloud height is about 1.25 km lower than the Cloudnet cloud top height, with a standard deviation of 2.31 km.

Figure 7b shows the histogram results for 1 km bins of the Cloudnet cloud middle height and the SCIAMACHY cloud height products. The number of data in each bin is different from Fig. 7a, because a Cloudnet cloud can fall into a different bin by considering the cloud top height or the cloud middle height. The FRESCO cloud height has a good agreement with the Cloudnet cloud middle height for 85 % of the cases and for the bins from 0–6 km. The smallest difference of 0.01 km occurs in the 2–3 km bin. The mean difference between the FRESCO cloud height and the Cloudnet cloud middle height is only −0.14 km, with a standard deviation of 1.88 km. The values that are used in Fig. 7 are provided in Tables A1–A4 of the Appendix.

4.2.2 Multi-layer clouds

Both the FRESCO and SACURA algorithm assume a single layer cloud in the retrieval model. In case of two-layer cloud systems, the FRESCO cloud height is located between the two cloud layers and closest to the optically thicker layer (Wang et al., 2008, 2012; Sneep et al., 2008). The SACURA algorithm retrieves a cloud top height close to the cloud top of the lower cloud if the high cloud is optically thin. If the optical thickness of the high cloud layer is larger than 6, SACURA most likely retrieves a cloud top height higher than the top of the high cloud (Lelli et al., 2012). This behaviour is also expected in the current comparison. Figure 8 shows the scatter plots of FRESCO cloud height vs. Cloudnet cloud top height and Cloudnet cloud middle height, respectively, for multi-layer cloud cases. The FRESCO cloud height is indeed closer to the Cloudnet cloud middle height than to the cloud top height, especially for low multi-layer clouds. Similar to the single-layer cloud cases, the FRESCO cloud height can be too high (at 15 km) for clouds with effective cloud fraction below 0.1.

AMTD
6, 8603–8645, 2013

The scatter plots of the ESA L2 cloud top height vs. the Cloudnet cloud top height and cloud middle height for multi-layer cloud cases (Fig. 9) show more spread than for single-layer cloud cases (cf. Fig. 5). However, the data points are distributed almost symmetrically along the one-to-one line. The ESA L2 cloud top height is in general higher than the Cloudnet cloud middle height.

The cloud height distributions of multi-layer clouds are shown in Fig. 10, as the multi-layer analogue of Fig. 6. Here the cases are sorted according to the Cloudnet cloud middle height. The Cloudnet cloud height distribution, indicated by blue-white colours, is normalized to 1 using the maximum occurrence frequency (because of the different temporal and vertical resolutions of the data at Cabauw and Lindenberg, the absolute number of occurrences is different for the two sites). The occurrence frequency can be understood as the relative cloud fraction per altitude bins. The frequency of 1 means fully cloudy. A larger occurrence frequency and a wider distribution indicate more clouds at certain altitudes, which correspond to large cloud fraction and geometrically thick clouds. As shown in Fig. 10, the FRESCO cloud height agrees well with the peak height of the cloud distribution, up to 5 km. For higher peak heights, the FRESCO cloud height is closer to the lower cloud layers. Most of the FRESCO cloud heights are inside the Cloudnet cloud height distributions. For multi-layer clouds Fig. 10 shows that the ESA L2 cloud top height is generally higher than the FRESCO cloud height and lower than the Cloudnet cloud top height, but it does not show a clear relation with the Cloudnet cloud height distribution.

Similar to the single-layer cloud cases, the cloud heights for multi-layer clouds have also been divided into height bins according to the Cloudnet cloud top height and cloud middle height, respectively. The results are presented in Fig. 11. The cloud top heights of multi-layer clouds are usually higher than those of single-layer clouds. It appears that the FRESCO cloud height is close to the Cloudnet cloud top height for multi-layer low clouds, but we note that only a small percentage of low clouds are multi-layer cloud cases: 19 % for the cloud top height bins and or 28 % cloud middle height bins. Here low clouds refer to clouds in the bins 1–3. The ESA L2 cloud top height for multi-layer

AMTD
6, 8603–8645, 2013

clouds has about 37 % of cases close to the Cloudnet cloud top height within 1 km; however, the standard deviation of the ESA L2 cloud top height is about 2–4 km, which is rather large.

Comparing Fig. 11 to Fig. 7, the FRESCO cloud height and ESA L2 cloud top height behave consistently for single-layer and multi-layer clouds. However, for the multi-layer cloud cases, the differences between SCIAMACHY cloud heights and Cloudnet cloud top and middle heights have larger standard deviations than for single-layer cloud cases.

When we divide the Cloudnet cloud top heights into low, middle and high clouds using separation levels at 3 and 6 km, there are 158 (37.5 %) low clouds, 88 (20.9 %) middle clouds and 175 (41.6 %) high clouds out of 421 single- and multi-layer cloud cases in this validation data set. The percentages are comparable to those reported by Stubenrauch et al. (2012). The mean differences that we find between the SCIAMACHY cloud heights and the Cloudnet cloud height for all cloud cases may not be representative for the global mean differences. However, the cloud height comparisons for every 1 km height bin can be considered valid globally, if the clouds are classified in the proper bin. More statistics of the comparison between SCIAMACHY cloud heights and Cloudnet cloud heights for multi-layer clouds is given in the Appendix in Tables A5–A8.

5 Conclusions

Two SCIAMACHY O_2 A band cloud height products, FRESCO (version 6) and ESA L2 (version 5.02), have been validated using the Cloudnet radar/lidar classification and cloud boundaries at Cabauw and Lindenberg, from January 2003 to December 2011. The collocated cases are separated into single-layer clouds and multi-layer clouds according to the height distribution of the radar/lidar backscatter signals in one hour around the SCIAMACHY overpass time. We found in total 693 collocated cases. After

AMTD
6, 8603–8645, 2013

excluding the cases with (effective) cloud fractions smaller than 0.1, 421 cases remain, of which 217 cases are single-layer clouds and 204 cases are multi-layer clouds.

The FRESCO cloud height appears to be close to the Cloudnet cloud middle height for both single-layer and multi-layer clouds. The ESA L2 cloud top height appears to be close to the Cloudnet cloud top height for middle level clouds, higher than the Cloudnet cloud top height for low clouds and lower than the Cloudnet cloud top height for high clouds. This agrees with the finding by Lelli et al. (2012) for GOME cloud heights. Statistics of the validation are analyzed for single-layer clouds and multi-layer clouds for 1 km height bins. The differences are quantified in detail due to the relatively large validation data set. Therefore we can conclude that the FRESCO cloud height is accurate as a cloud middle height for clouds below 5 km and the ESA L2 cloud top height is on average reliable as a cloud top height for clouds at 3–7 km, but it has a large scatter.

Because of a limited number of ground-based radar/lidar measurement sites worldwide, it is not possible to validate the SCIAMACHY cloud products globally. In the validation data set for Cabauw and Lindenberg, there appear to be more low clouds than high clouds (including high clouds on top of low clouds). This leads to a larger percentage of FRESCO cloud heights close to the Cloudnet measurements, while the percentage of results for the ESA L2 cloud top height is smaller. However, from the global FRESCO cloud height distribution and ESA L2 cloud top height distribution from the SCIAMACHY data set, covering all latitudes and all months, it appears that both cloud height products show more low clouds than high clouds. Based on other satellite cloud height products, globally 42 % of all clouds are high clouds, and about 42 % of all clouds are single-layer low-level clouds (Stubenrauch et al., 2012). We may conclude that as a global cloud product, FRESCO cloud height is accurate for low clouds, whereas the ESA L2 cloud top height is more accurate for middle level clouds.

The cloud height distributions at Cabauw and Lindenberg, where the SCIAMACHY cloud height validation has been performed, cannot be considered as being representative for the entire globe. However, the validation results of this paper in terms of the reported accuracy of the SCIAMACHY cloud product per 1 km height bin can be trans-

AMTD
6, 8603–8645, 2013

lated into an estimate of the SCIAMACHY cloud height accuracy at other locations in the world. For such an estimate the true (or climatologically) vertical distribution of clouds at other locations would be required.

Acknowledgements. We thank our KNMI colleagues Ronald van der A for processing FRESCO data and Henk Klein Baltink for help with Cloudnet data. We acknowledge ESA for the provision of SCIAMACHY L1 and L2 data. We acknowledge the Cloudnet project (European Union contract EVK2-2000-00611) for providing the Target Classification product, which was produced by the University of Reading and KNMI using measurements from the Cabauw Experimental Site for Atmospheric Research (CESAR), and DWD (German Weather Service) using measurements from the Lindenberg site. This work was supported by the Netherlands Space Office (NSO) as part of the SCIA-Visie project.

References

Anderson, G. P., Clough, S. A., Kneizys, F. X., Chetwynd, J. H., and Shettle, E. P.: AFGL atmospheric constituent profiles, Tech. Rep. AFGL-TR-86-0110, Air Force Geophys. Lab., Hanscom AFB, MA, 1986.

Boersma, K. F., Eskes, H. J., and Brinksma, E. J.: Error analysis for tropospheric NO_2 retrieval from space, J. Geophys. Res., 109, D04311, doi:10.1029/2003JD003962, 2004.

Bovensmann, H., Burrows, J. P., Buchwitz, M., Frerick, J., Noel, S., Rozanov, V. V., Chance, K. V., and Goede, A. P. H.: SCIAMACHY: mission objectives and measurement modes, J. Atmos. Sci., 56, 127–150, 1999.

Buchwitz, M., Rozanov, V. V., and Burrows, J. P.: A correlated *k* distribution scheme for overlapping gases suitable for retrieval of atmospheric constituents from moderate resolution radiance measurements in the visible/near-infrared spectral region, J. Geophys. Res., 105, 15247–15262, 2000.

Feigelson, E. M. (Ed.): Radiation in a Cloudy Atmosphere, Gidrometeoizdat, Leningrad, 280 pp., 1981.

Ferlay, N., Thieuleux, F., Cornet, C., Davis, A. B., Dubuisson, P., Ducos, F., Parol, F., Riedi, J., and Vanbauce, C.: Toward new inferences about cloud structures from multidirectional measurements in the oxygen A band: middle-of cloud pressure and cloud ge-

AMTD
6, 8603–8645, 2013

Validation of SCIAMACHY O_2 A band cloud heights

P. Wang and P. Stammes

ometrical thickness from POLDER-3/PARASOL, J. Appl. Meteorol. Clim., 49, 2492–2507, doi:10.1175/2010JAMC2550.1, 2010.
Hogan, R. J. and O'Connor, E. J.: Facilitating cloud radar and lidar algorithms: the Cloudnet Instrument Synergy/Target Categorization product, available at: http://www.met.rdg.ac.uk/~swrhgnrj/publications/categorization.pdf (last access: 30 September 2013), 2004.
Illingworth, A. J., Hogan, R. J., O'Connor, E. J., Bouniol, D., Brooks, M. E., Delanoe, J., Donovan, D. P., Eastment, J. D., Gaussiat, N., Goddard, J. W. F., Haeffelin, M., Klein Baltink, H., Krasnov, O. A., Pelon, J., Piriou, J.-M., Protat, A., Russchenberg, H. W. J., Seifert, A., Tompkins, A. M., van Zadelhoff, G.-J., Vinit, F., Willen, U., Wilson, D. R., and Wrench, C. L.: Cloudnet – continuous evaluation of cloud profiles in seven operational models using ground-based observations, B. Am. Meteorol. Soc., 88, 883–898, 2007.
Koelemeijer, R. B. A., Stammes, P., Hovenier, J. W., and de Haan, J. F.: A fast method for retrieval of cloud parameters using oxygen A band measurements from the Global Ozone Monitoring Experiment, J. Geophys. Res., 106, 3475–3490, 2001.
Kokhanovsky, A. A., Rozanov, V. V., Nauss, T., Reudenbach, C., Daniel, J. S., Miller, H. L., and Burrows, J. P.: The semi-analytical cloud retrieval algorithm for SCIAMACHY. I. The validation, Atmos. Chem. Phys., 6, 1905–1911, 2006, http://www.atmos-chem-phys.net/6/1905/2006/.
Kokhanovsky, A. A., Nauss, T., Schreier, M., von Hoyningen-Huene, W., and Burrows, J. P.: The intercomparison of cloud parameters derived using multiple satellite instruments, IEEE Trans. Geosci. Remote, 45, 195–200, doi:10.1109/TGRS.2006.885019, 2007.
Krijger, J. M., van Weele, M., Aben, I., and Frey, R.: Technical Note: The effect of sensor resolution on the number of cloud-free observations from space, Atmos. Chem. Phys., 7, 2881–2891, 2007, http://www.atmos-chem-phys.net/7/2881/2007/.
Lelli, L., Kokhanovsky, A. A., Rozanov, V. V., Vountas, M., Sayer, A. M., and Burrows, J. P.: Seven years of global retrieval of cloud properties using space-borne data of GOME, Atmos. Meas. Tech., 5, 1551–1570, doi:10.5194/amt-5-1551-2012, 2012.
Lichtenberg, G.: Verification Report OL V 5.0, SCIAMACHY Level 1b to 2 processing, ENV-VPR-QWG-SCIA-0095, Issue 2, 15 June 2009, available at: http://atmos.caf.dlr.de/sciamachy/documents/level_1b_2/SCIAVerification_L12_OL5.pdf (last access: 30 September 2013), 2009.

AMTD
6, 8603–8645, 2013

Validation of SCIAMACHY O_2 A band cloud heights

P. Wang and P. Stammes

Lichtenberg, G.: SCIAMACHY Offline Processor Level1b-2 ATBD, Algorithm Theoretical Baseline Document (SGP OL Version 5), 23 March 2011, available at: http://atmos.caf.dlr.de/sciamachy/documents/level_1b_2/sciaol1b2_atbd_master.pdf (last access: 30 September 2013), 2011.

Loyola, D. G.: Automatic cloud analysis from polar orbiting satellites using neural network and data fusion techniques, IEEE T. Geosci. Remote, 4, 2530–2534, doi:10.1109/IGARSS.2004.1369811, 2004.

Popp, C., Wang, P., Brunner, D., Stammes, P., Zhou, Y., and Grzegorski, M.: MERIS albedo climatology for FRESCO+ O_2 A band cloud retrieval, Atmos. Meas. Tech., 4, 463–483, 2011, http://www.atmos-meas-tech.net/4/463/2011/.

Rothman, L. S., Gordon, I. E., Barbe, A., Benner, D. C., Bernath, P. F., Birk, M., Boudon, V., Brown, L. R., Campargue, A., Champion, J.-P., Chance, K., Coudert, L. H., Dana, V., Devi, V. M., Fally, S., Flaud, J.-M., Gamache, R. R., Goldman, A., Jacquemart, D., Kleiner, I., Lacome, N., Lafferty, W. J., Mandin, J.-Y., Massie, S. T., Mikhailenko, S. N., Miller, C. E., Moazzen-Ahmadi, N., Naumenko, O. V., Nikitin, A. V., Orphal, J., Perevalov, V. I., Perrin, A., Predoi-Cross, A., Rinsland, C. P., Rotger, M., Simeckova, M., Smith, M. A. H., Sung, K., Tashkun, S. A., Tennyson, J., Toth, R. A., Vandaele, A. C., and Vander Auwera, J.: The HITRAN 2008 molecular spectroscopic database, J. Quant. Spectrosc. Ra., 110, 533–572, 2009.

Rozanov, V. V. and Kokhanovsky, A. A.: Semianalytical cloud retrieval algorithm as applied to the cloud top altitude and the cloud geometrical thickness determination from top-of-atmosphere reflectance measurements in the oxygen A band, J. Geophys. Res., 109, 5202, doi:10.1029/2003JD004104, 2004.

Rozanov, V. V., Kokhanovsky, A. A., Loyola, D. G., Siddans, R., Latter, B., Stevens, A., and Burrows, J. P.: Intercomparison of cloud top altitudes as derived using GOME and ATSR-2 instruments onboard ERS-2, Remote Sens. Environ., 102, 186–193, doi:10.1109/TGRS.2004.825586, 2006.

Sayer, A. M., Poulsen, C. A., Arnold, C., Campmany, E., Dean, S., Ewen, G. B. L., Grainger, R. G., Lawrence, B. N., Siddans, R., Thomas, G. E., and Watts, P. D.: Global retrieval of ATSR cloud parameters and evaluation (GRAPE): dataset assessment, Atmos. Chem. Phys., 11, 3913–3936, doi:10.5194/acp-11-3913-2011, 2011.

Sneep, M., de Haan, J. F., Stammes, P., Wang, P., Vanbauce, C., Joiner, J., Vasilkov, A. P., and Levelt, P. F.: Three-way comparison between OMI and PARASOL cloud pressure products, J. Geophys. Res., 113, D15S23, doi:10.1029/2007JD008694, 2008.

Stammes, P., Sneep, M., de Haan, J. F., Veefkind, J. P., Wang, P., and Levelt, P. F.: Effective cloud fractions from the Ozone Monitoring Instrument: theoretical framework and validation, J. Geophys. Res., 113, D16S38, doi:10.1029/2007JD008820, 2008.

Stubenrauch, C. J., Rossow, W. B., Kinne, S., Ackerman, S., Cesana, G., Chepfer, H., Di Girolamo, L., Getzewich, B., Guignard, A., Heidinger, A., Maddux, B., Menzel, P., Minnis, P., Pearl, C., Platnick, S., Poulsen, C., Riedi, J., Sun-Mack, S., Walther, A., Winker, D., Zeng, S., Zhao, G.: Assessment of global cloud datasets from satellites: project and database initiated by the GEWEX Radiation Panel, B. Am. Meteorol. Soc., 94, 1031–1049, doi:10.1175/BAMS-D-12-00117, 2012.

Wang, P., Stammes, P., van der A, R., Pinardi, G., and van Roozendael, M.: FRESCO+: an improved O_2 A band cloud retrieval algorithm for tropospheric trace gas retrievals, Atmos. Chem. Phys., 8, 6565–6576, doi:10.5194/acp-8-6565-2008, 2008.

Wang, P., Tuinder, O. N. E., Tilstra, L. G., de Graaf, M., and Stammes, P.: Interpretation of FRESCO cloud retrievals in case of absorbing aerosol events, Atmos. Chem. Phys., 12, 9057–9077, doi:10.5194/acp-12-9057-2012, 2012.

Wielicki, B. A., Wong, T., Loeb, N., Minnis, P., Priestley, K., and Kande, R.: Changes in Earth's albedo measured by satellite, Science, 308, p. 825, doi:10.1126/science.1106484, 2005.

Winker, D., Vaughan, M., Omar, A., Hu, Y., Powell, K., Liu, Z., Hunt, W., and Young, S.: Overview of the CALIPSO mission and CALIOP data processing algorithm, J. Atmos. Ocean. Tech., 26, 2310–2323, 2009.

Table 1. Information on the Cloudnet target classification product at Cabauw and Lindenberg.

	Latitude (° N)	Longitude (° E)	Surface height (m)	Time resolution (s)	Altitude range (m)	Altitude grid (m)	Time period
Cabauw	51.97	4.93	−0.7	15	253–11 500	90	January 2003–June 2005
Lindenberg	52.21	14.13	103.0	30	324–15 000	30	January 2005–December 2011

AMTD
6, 8603–8645, 2013

Validation of SCIAMACHY O_2 A band cloud heights

P. Wang and P. Stammes

Table 2. Statistics of SCIAMACHY FRESCO (v6) and ESA L2 (v5.02) global cloud products, σ = standard deviation.

	Effective cloud fraction			Cloud (top) height (km)			
	Mean	σ	No. of data	Mean	σ	No. of data	Time period
FRESCO (v6)	0.348	0.302	924 335	3.53	2.54	630 404	August 2002–April 2012
ESA L2 (v5.02)	0.326	0.314	924 335	4.14	3.53	630 404	
FRESCO-ESA	0.0225	0.100	924 335	−0.609	2.16	630 404	

AMTD
6, 8603–8645, 2013

Table A1. Comparison of SCIAMACHY FRESCO cloud height with Cloudnet cloud top height for single-layer clouds.

Cloud top bins (km)	Cloudnet cloud top height (km)		FRESCO cloud height (km)		FRESCO – Cloudnet (km)		No. of cases
–	mean	stddev	mean	stddev	mean	stddev	
0–1	0.79	0.15	1.19	0.67	0.40	0.65	14
1–2	1.54	0.24	1.74	0.98	0.20	1.01	68
2–3	2.46	0.29	2.05	0.65	−0.41	0.70	38
3–4	3.47	0.24	2.90	0.92	−0.57	0.81	14
4–5	4.35	0.31	2.44	0.69	−1.90	0.76	9
5–6	5.45	0.33	3.75	1.28	−1.70	1.39	14
6–7	6.48	0.26	3.12	1.26	−3.36	1.27	11
7–8	7.63	0.35	5.74	4.06	−1.89	4.09	9
8–10	9.03	0.58	5.04	1.72	−3.99	1.96	25
> 10	10.60	0.33	5.75	3.01	−4.85	2.99	15
All	4.14	3.17	2.89	2.10	−1.25	2.31	217

AMTD

6, 8603–8645, 2013

Validation of SCIAMACHY O_2 A band cloud heights

P. Wang and P. Stammes

Table A2. Comparison of ESA L2 cloud top height with Cloudnet cloud top height for single-layer clouds.

Cloud top bins (km)	Cloudnet top height (km)		ESA L2 cloud top height (km)		ESA L2 – Cloudnet (km)		No. of cases
–	mean	stddev	mean	stddev	mean	stddev	
0–1	0.75	0.16	2.24	2.42	1.49	2.40	9
1–2	1.53	0.23	2.95	1.97	1.42	1.98	54
2–3	2.49	0.29	4.77	3.04	2.28	3.05	33
3–4	3.43	0.24	4.15	1.02	0.72	1.14	12
4–5	4.31	0.31	4.27	2.17	–0.04	2.16	8
5–6	5.40	0.30	5.66	1.86	0.25	1.93	13
6–7	6.50	0.26	6.15	4.33	–0.35	4.48	9
7–8	7.62	0.39	4.47	2.61	–3.15	2.69	7
8–10	9.00	0.62	6.77	2.82	–2.23	3.02	21
> 10	10.47	0.32	6.93	2.77	–3.54	2.81	8
All	4.03	3.00	4.47	2.86	0.44	3.07	174

AMTD
6, 8603–8645, 2013

Validation of SCIAMACHY O_2 A band cloud heights

P. Wang and P. Stammes

Table A3. Comparison of SCIAMACHY FRESCO cloud height with Cloudnet cloud middle height for single-layer clouds.

Cloud middle bins (km)	Cloudnet middle height (km)		FRESCO cloud height (km)		FRESCO – Cloudnet (km)		No. of cases
–	mean	stddev	mean	stddev	mean	stddev	
0–1	0.73	0.15	1.64	1.42	0.91	1.37	21
1–2	1.42	0.29	1.81	0.81	0.39	0.77	90
2–3	2.50	0.32	2.51	0.80	0.01	0.79	27
3–4	3.55	0.27	3.47	1.24	−0.09	1.20	24
4–5	4.52	0.32	4.40	1.61	−0.12	1.56	11
5–6	5.37	0.27	4.43	1.86	−0.95	1.88	11
6–7	6.33	0.27	4.78	1.98	−1.55	2.02	17
7–8	7.32	0.25	7.82	4.93	0.49	4.80	4
8–10	8.66	0.43	6.08	2.94	−2.58	3.18	6
> 10	10.34	0.33	5.33	4.54	−5.01	4.60	6
All	3.02	2.39	2.89	2.10	−0.14	1.88	217

AMTD
6, 8603–8645, 2013

Validation of SCIAMACHY O_2 A band cloud heights

P. Wang and P. Stammes

Table A4. Comparison of SCIAMACHY ESA L2 cloud top height with Cloudnet cloud middle height for single-layer clouds.

Cloud middle bins (km)	Cloudnet middle height (km)		ESA L2 cloud top height (km)		ESA L2 – Cloudnet (km)		No. of cases
–	mean	stddev	mean	stddev	mean	stddev	
0–1	0.70	0.16	2.53	2.52	1.83	2.50	15
1–2	1.40	0.28	3.38	1.95	1.97	1.87	74
2–3	2.53	0.32	5.14	3.08	2.61	3.13	25
3–4	3.56	0.24	5.61	3.28	2.05	3.19	21
4–5	4.48	0.30	6.07	0.96	1.59	0.87	10
5–6	5.36	0.28	6.16	1.97	0.80	1.96	10
6–7	6.36	0.28	6.60	2.49	0.24	2.56	14
7–8	7.11	0.03	5.23	1.83	−1.89	1.87	2
8–10	8.62	0.70	9.08	11.21	0.46	11.90	2
> 10	10.34	–	1.15	–	−9.19	–	1
All	2.77	1.97	4.47	2.86	1.71	2.71	174

Discussion Paper | Discussion Paper | Discussion Paper | Discussion Paper |

AMTD

6, 8603–8645, 2013

Validation of SCIAMACHY O_2 A band cloud heights

P. Wang and P. Stammes

Table A5. Comparison of SCIAMACHY FRESCO cloud height with Cloudnet cloud top height for multi-layer clouds.

Cloud top bins (km)	Cloudnet cloud top height (km)		FRESCO cloud height (km)		FRESCO – Cloudnet (km)		No. of cases
–	mean	stddev	mean	stddev	mean	stddev	
0–1	0.92	0.07	0.78	0.21	−0.14	0.13	2
1–2	1.47	0.35	1.88	0.77	0.42	0.64	14
2–3	2.50	0.35	2.11	1.02	−0.39	0.97	22
3–4	3.54	0.38	2.05	0.94	−1.50	1.08	18
4–5	4.61	0.23	2.76	1.32	−1.85	1.33	15
5–6	5.54	0.28	2.89	1.25	−2.65	1.28	18
6–7	6.48	0.29	2.79	1.19	−3.68	1.20	24
7–8	7.58	0.31	3.63	1.77	−3.95	1.73	27
8–10	8.91	0.57	4.20	2.28	−4.71	2.43	47
> 10	10.80	0.44	5.20	2.74	−5.60	2.57	17
All	6.24	2.84	3.21	1.96	−3.02	2.50	204

AMTD
6, 8603–8645, 2013

Validation of SCIAMACHY O_2 A band cloud heights

P. Wang and P. Stammes

Table A6. Comparison of SCIAMACHY ESA L2 cloud top height with Cloudnet cloud top height for multi-layer clouds.

Cloud top bins (km)	Cloudnet cloud top height (km)		ESA L2 cloud top height (km)		ESA L2 – Cloudnet (km)		No. of cases
–	mean	stddev	mean	stddev	mean	stddev	
0–1	0.92	0.07	1.13	0.03	0.21	0.11	2
1–2	1.44	0.34	4.42	3.62	2.99	3.53	13
2–3	2.49	0.36	3.81	3.20	1.32	3.26	18
3–4	3.52	0.39	3.83	2.18	0.32	2.16	14
4–5	4.56	0.27	4.66	2.28	0.10	2.16	13
5–6	5.56	0.26	5.31	2.99	–0.25	3.02	13
6–7	6.43	0.29	7.10	4.66	0.67	4.69	21
7–8	7.59	0.33	5.07	2.95	–2.52	2.96	22
8–10	8.92	0.60	6.39	3.94	–2.52	4.05	40
> 10	10.75	0.40	8.88	3.93	–1.87	4.08	14
All	6.21	2.87	5.60	3.76	–0.61	3.91	170

AMTD
6, 8603–8645, 2013

Validation of SCIAMACHY O_2 A band cloud heights

P. Wang and P. Stammes

Table A7. Comparison of SCIAMACHY FRESCO cloud height with Cloudnet cloud middle layer height for multi-layer clouds.

Cloud middle bins (km)	Cloudnet cloud middle height (km)		FRESCO cloud height (km)		FRESCO – Cloudnet (km)		No. of cases
–	mean	stddev	mean	stddev	mean	stddev	–
0–1	0.81	0.11	1.17	0.56	0.36	0.60	8
1–2	1.58	0.27	1.92	0.58	0.34	0.73	23
2–3	2.42	0.30	2.49	1.23	0.07	1.24	27
3–4	3.57	0.26	2.75	1.03	−0.82	1.01	22
4–5	4.46	0.30	2.82	1.22	−1.65	1.21	37
5–6	5.45	0.31	3.67	1.90	−1.78	1.98	39
6–7	6.41	0.25	4.26	1.88	−2.15	1.86	19
7–8	7.43	0.32	5.28	2.62	−2.14	2.71	16
8–10	8.59	0.49	4.01	1.95	−4.58	2.10	12
> 10	10.32	–	13.76	–	3.44	–	1
All	4.50	2.15	3.21	1.96	−1.29	2.02	204

AMTD
6, 8603–8645, 2013

Validation of SCIAMACHY O_2 A band cloud heights

P. Wang and P. Stammes

Table A8. Comparison of SCIAMACHY ESA L2 cloud top height with Cloudnet cloud middle height for multi-layer clouds.

Cloud middle bins (km)	Cloudnet cloud middle height (km)		ESA L2 cloud top height (km)		ESA L2 – Cloudnet (km)		No. of cases
–	mean	stddev	mean	stddev	mean	stddev	–
0–1	0.81	0.12	2.27	2.48	1.46	2.51	8
1–2	1.58	0.26	4.21	3.48	2.63	3.56	21
2–3	2.45	0.29	4.13	2.18	1.69	2.08	22
3–4	3.58	0.27	5.16	3.00	1.59	2.96	19
4–5	4.44	0.29	5.06	3.09	0.63	3.10	29
5–6	5.46	0.31	6.38	3.83	0.92	3.86	38
6–7	6.40	0.24	6.88	3.66	0.48	3.63	13
7–8	7.37	0.29	9.56	4.12	2.19	4.19	11
8–10	8.68	0.53	8.07	5.47	−0.61	5.64	9
> 10	–	–	–	–	–	–	0
All	4.35	2.09	5.60	3.76	1.25	3.50	170

Discussion Paper | Discussion Paper | Discussion Paper | Discussion Paper |

AMTD

6, 8603–8645, 2013

Validation of SCIAMACHY O_2 A band cloud heights

P. Wang and P. Stammes

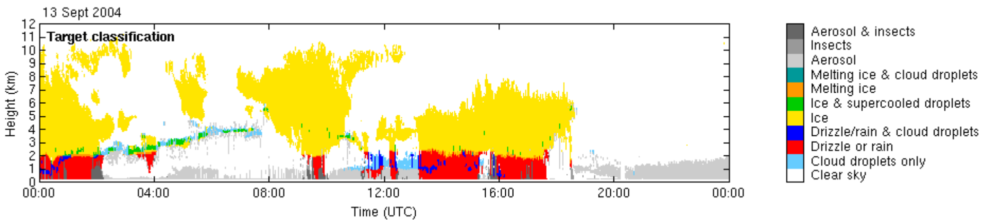

Fig. 1. Quick-look image of the Cloudnet target classification product at Lindenberg on 13 September 2004 (downloaded from www.cloud-net.org).

AMTD
6, 8603–8645, 2013

Validation of SCIAMACHY O_2 A band cloud heights

P. Wang and P. Stammes

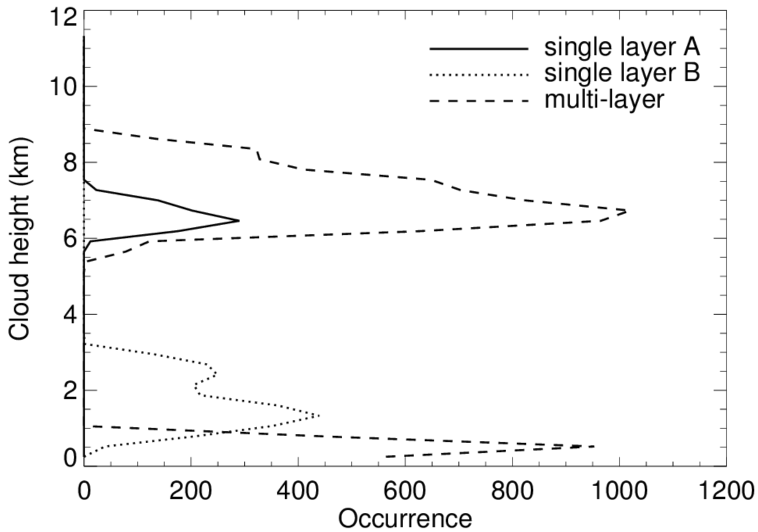

Fig. 2. Three examples of Cloudnet cloud vertical distributions: two single-layer cases and one multi-layer case. The distributions are based on one-hour data centered at the SCIAMACHY overpass time (about 10:00 LT).

AMTD
6, 8603–8645, 2013

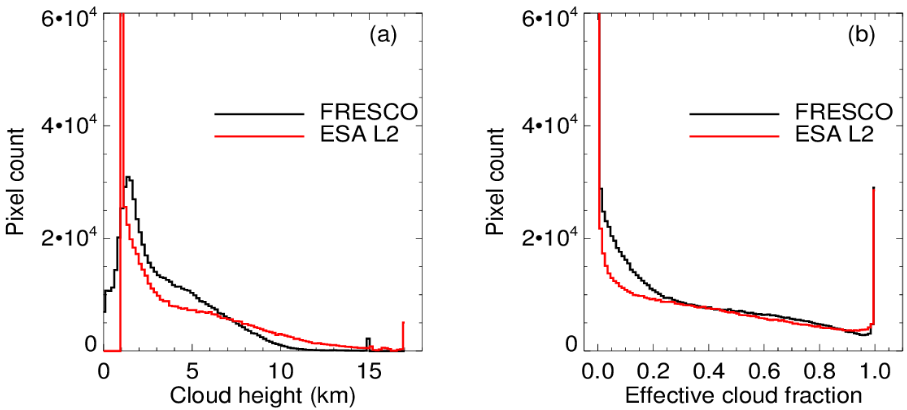

Fig. 3. (a) Global distribution of SCIAMACHY FRESCO cloud height and ESA L2 cloud top height. **(b)** Global distribution of SCIAMACHY FRESCO effective cloud fraction and ESA L2 cloud fraction. The pixel count for the ESA L2 product (out of range in the plots) is 1.6×10^5 at cloud height of 1 km in **(a)** and is 2.0×10^5 at effective cloud fraction of 0.0 in **(b)**.

AMTD
6, 8603–8645, 2013

P. Wang and P. Stammes

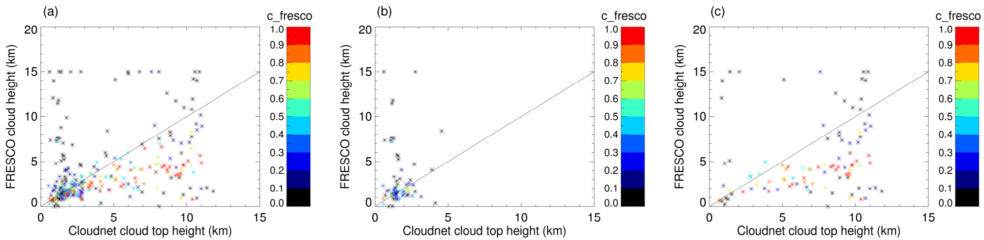

Fig. 4. Scatter plot of SCIAMACHY FRESCO cloud height vs. Cloudnet cloud top height, for **(a)** all single-layer clouds, **(b)** single-layer water clouds, **(c)** single-layer ice clouds. The color of the symbol indicates the FRESCO effective cloud fraction, with the color code given by the vertical bar. The black line is the one-to-one line. For the points with c_fresco > 0.1, the correlation coefficients are **(a)** 0.685, **(b)** 0.206, and **(c)** 0.489. The linear relationship is significant in **(a)** and **(c)** but not in **(b)**.

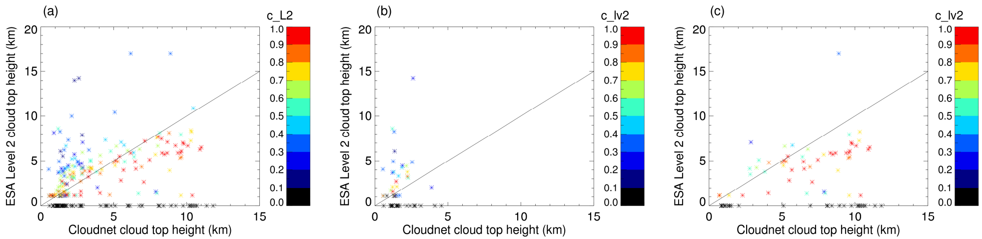

Fig. 5. Scatter plot of SCIAMACHY ESA L2 cloud top height versus Cloudnet cloud top height, for **(a)** all single-layer clouds, **(b)** single-layer water clouds, **(c)** single-layer ice clouds. The color of the symbol indicates the ESA L2 cloud fraction, with the color code given by the vertical bar. The black line is the one-to-one line. For the points with c_lv2 > 0.1, the correlation coefficients are **(a)** 0.451, **(b)** 0.247, and **(c)** 0.426. The linear relationship is significant in **(a)** and **(c)** but not in **(b)**.

AMTD
6, 8603–8645, 2013

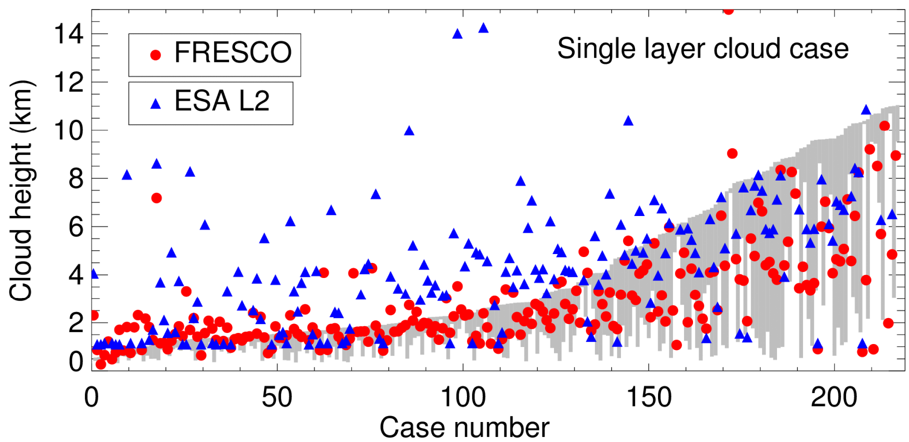

Fig. 6. Comparison between SCIAMACHY ESA L2 cloud top height, FRESCO cloud height, and Cloudnet cloud top and cloud base height for single-layer clouds. The cases are sorted according to the Cloudnet cloud top height. The grey bar indicates the altitude range of the cloud according to the Cloudnet product. Here the cases with FRESCO effective cloud fraction below 0.1 are excluded.

AMTD
6, 8603–8645, 2013

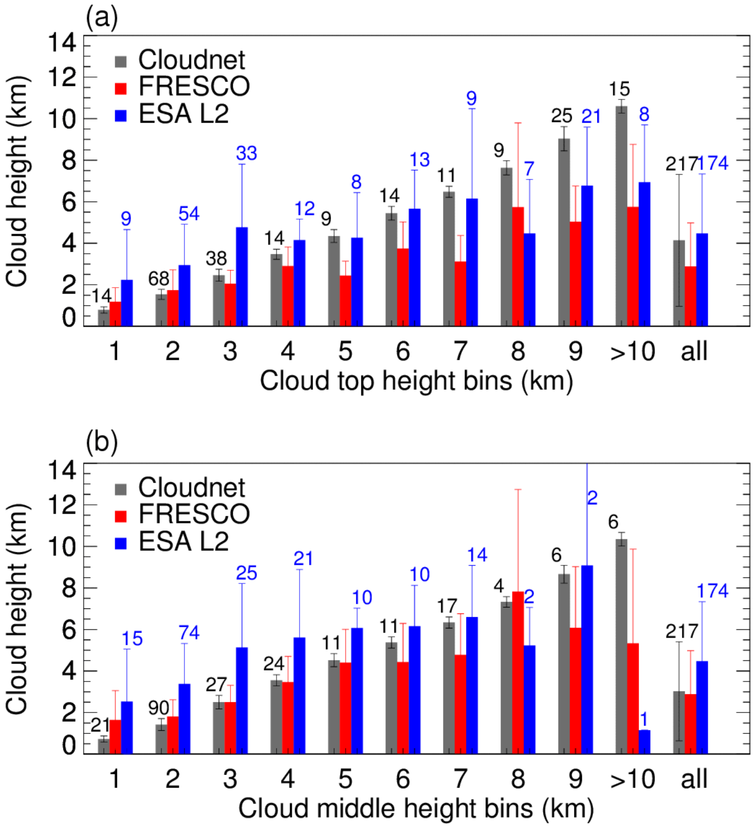

Fig. 7. (a) Histograms of Cloudnet cloud top height, FRESCO cloud height and ESA L2 cloud top height in 1 km bins of Cloudnet cloud top height, for single-layer clouds. The bins are 0–1, 1–2, ..., 7–8, 9–10 km, > 10 km and all cases. The number above the bar indicates the number of cases; the number of cases for FRESCO is the same as for Cloudnet. The error bar indicates the standard deviation of the data. **(b)** Same as **(a)** but for the Cloudnet cloud middle height bins.

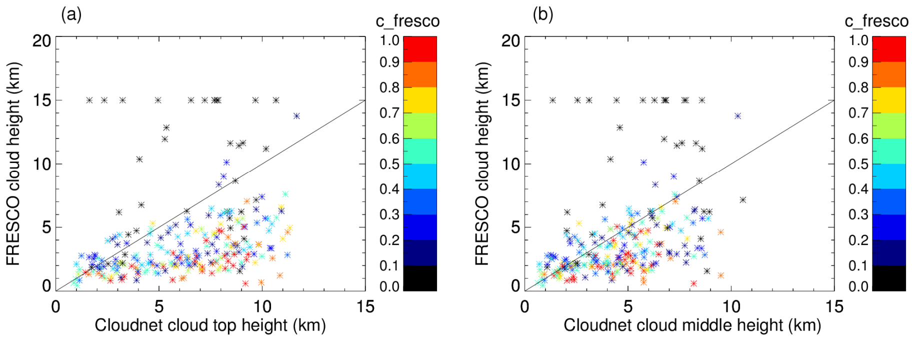

Fig. 8. (a) Scatter plot of SCIAMACHY FRESCO cloud height versus Cloudnet cloud top height, for multi-layer clouds. **(b)** Same as **(a)** but versus Cloudnet cloud middle height. The color of the symbol indicates the FRESCO effective cloud fraction, with the color code given by the vertical bar. The black line is the one-to-one line. For the points with c_fresco > 0.1, in **(a)** the correlation coefficient = 0.509; in **(b)** the correlation coefficient = 0.520. The linear relationship is significant in **(a)** and **(b)**.

AMTD
6, 8603–8645, 2013

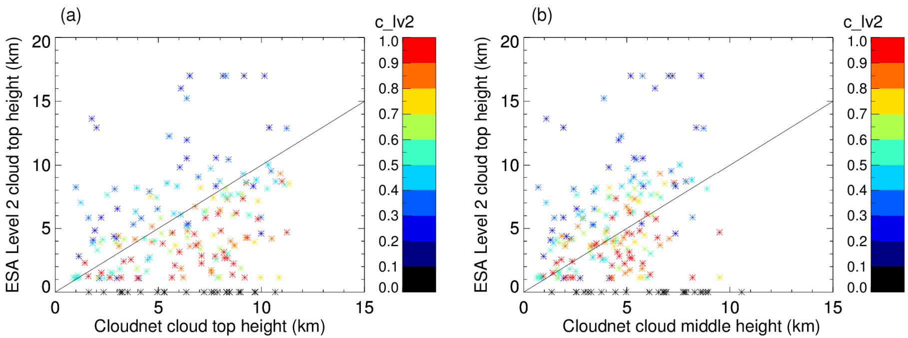

Fig. 9. (a) Scatter plot of ESA L2 cloud top height versus Cloudnet cloud top height, for multi-layer clouds. **(b)** Same as **(a)** but versus Cloudnet cloud middle height. The color of the symbol indicates the ESA L2 cloud fraction, with the color code given by the vertical bar. The black line is the one-to-one line. For the points with c_lv2 > 0.1, in **(a)** the correlation coefficient = 0.330; in **(b)** the correlation coefficient = 0.399. The linear relationship is significant in **(a)** and **(b)**.

AMTD
6, 8603–8645, 2013

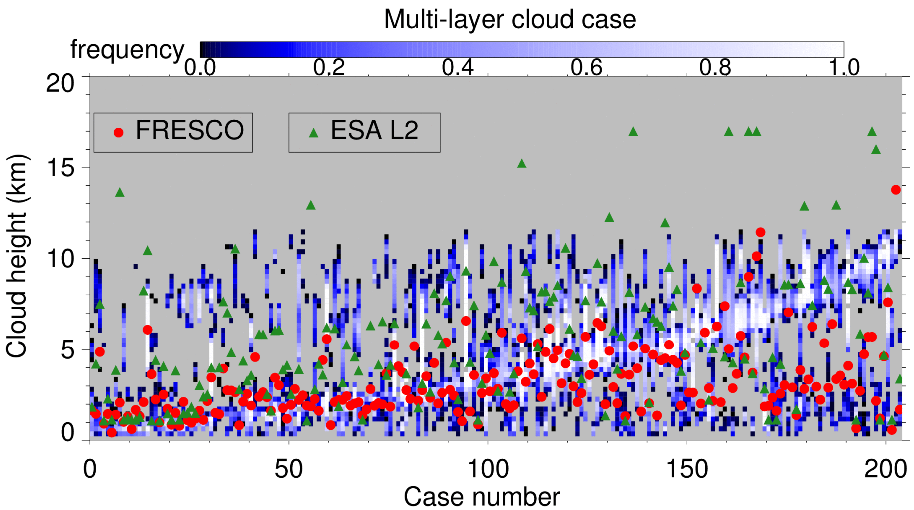

Fig. 10. Comparison between the SCIAMACHY ESA L2 cloud top height, the FRESCO cloud height, and the Cloudnet cloud height distribution. The cases are sorted according to the Cloudnet cloud middle height. The Cloudnet cloud height distribution is normalized to 1 and indicated with a blue-white color (color code given by the horizontal bar). Here the cases with FRESCO effective cloud fraction below 0.1 are excluded.

AMTD
6, 8603–8645, 2013

Validation of SCIAMACHY O_2 A band cloud heights

P. Wang and P. Stammes

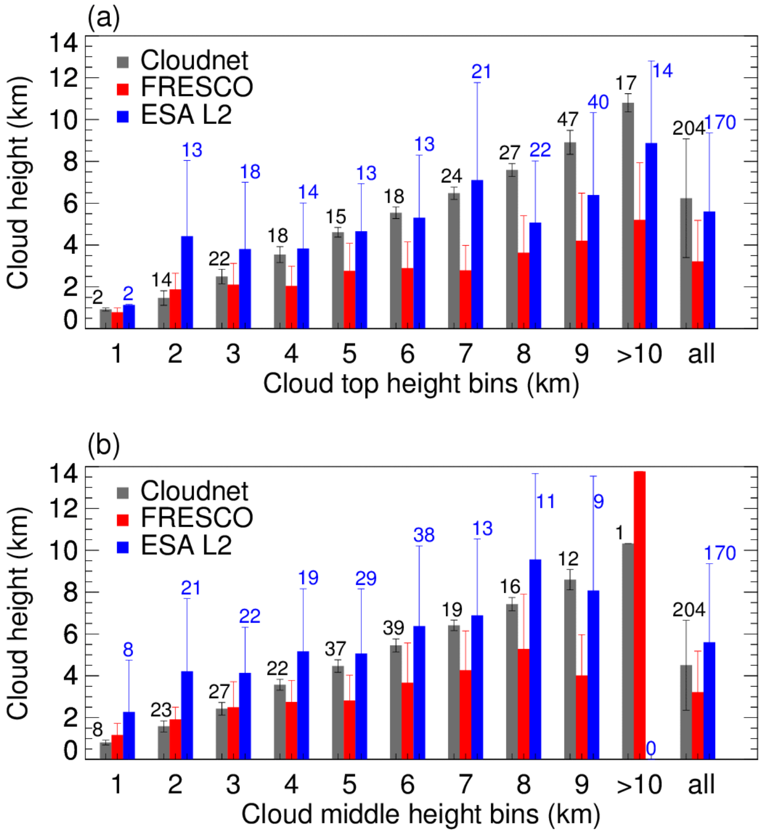

Fig. 11. (a) Histograms of Cloudnet cloud top height, FRESCO cloud height and ESA L2 cloud top height in 1 km bins of Cloudnet cloud top height, for multi-layer clouds. The bins are 0–1, 1–2, ..., 7–8, 9–10, > 10 km and all cases. The number above the bar indicates the number of cases; the number of cases for FRESCO is the same as for Cloudnet. The error bar indicates the standard deviation of the data. **(b)** Same as **(a)** but for the Cloudnet cloud middle height bins.

AMTD
6, 8603–8645, 2013

P. Wang and P. Stammes